

Microbunching Instability Suppression via Electron-Magnetic-Phase Mixing

S. Di Mitri^{1,*} and S. Spampinati^{1,2,3}

¹*Elettra—Sincrotrone Trieste, 34149, Basovizza (TS), Italy*

²*University of Liverpool, Department of Physics, Liverpool, United Kingdom*

³*Cockcroft Institute, Sci-Tech Daresbury, Warrington, United Kingdom*

(Received 5 December 2013; published 2 April 2014)

Control of the microbunching instability is a fundamental requirement in modern high-brightness electron linacs, in order to prevent misleading responses of beam optical diagnostics and contamination in the generation of coherent radiation, such as free electron lasers. We present the first experimental demonstration of control and suppression of microbunching instability by means of particles' longitudinal phase mixing in a magnetic chicane. In the presence of phase mixing, the intensity of the beam-emitted optical transition radiation, which is used as an indicator of the instability gain at optical wavelengths, is reduced by one order of magnitude and brought to the same level provided, alternatively, by beam heating. The experimental results are in agreement with particle tracking and analytical evaluations of the instability gain. This article is extended to a discussion of applications of magnetic-phase mixing to the generation of quasicold high-brightness ultrarelativistic electron beams.

DOI: 10.1103/PhysRevLett.112.134802

PACS numbers: 29.20.Ej, 29.27.Bd, 41.60.Cr

The understanding and control of electron beam energy and density modulations are vital for high-brightness linac-driven light sources such as free electron lasers (FELs). In the framework of the so-called microbunching instability [1–7], some undesired bunching—the Fourier transform of the longitudinal charge distribution and a measure of the density modulation amplitude—starts from electron beam shot noise and/or macroscopic density nonuniformities and is further amplified along the accelerator by the interplay of the longitudinal space charge (LSC) force, nonisochronous energy dispersive insertions and the emission of coherent synchrotron radiation (CSR). The strength of the microbunching instability is usually quantified by its spectral gain, which is the ratio of the final to the initial bunching [2–4]. When only LSC is considered, the gain can be evaluated by [1]

$$G(k) = Ck|R_{56}| \frac{I}{\gamma I_A} \frac{|Z(k)|}{Z_0} \exp\left(-\frac{1}{2}C^2k^2R_{56}^2\sigma_{\delta,0}^2\right), \quad (1)$$

where C is the electron bunch length compression factor provided by one magnetic insertion with momentum compaction R_{56} , k is the wave number of the energy modulation induced upstream of the compressor by the LSC impedance $Z(k)$, γ is the beam's relativistic Lorentz factor at the compressor, $\sigma_{\delta,0}$ is the beam fractional incoherent energy spread just before compression, $Z_0 = 377 \Omega$ and $I_A = 17045 \text{ A}$. In the following, the analytical gain in the presence of CSR, LSC and magnetic compression as depicted in [2–4] is considered. That is, the gain is the relative amplification factor of the initial density modulation and a gain smaller than 1 means that the additional modulation due to collective effects is smaller

than the modulation associated to the initial bunching. A maximum gain as large as 10^2 to 10^4 is common in linac-driven FELs and peaks at initial (i.e., before compression) wavelengths around few tens of micron [7–9]. Large bunching is accompanied by large energy modulation with analogous spectral content. The final energy modulation may act on the FEL process as large local (slice) energy spread that, depending also on the spatial scale of the cooperative FEL process, may reduce the FEL output power and/or enlarge the FEL spectral bandwidth [10–12]. A “laser heater” (LH) system was first proposed in [13] to counteract those disrupting effects. In a LH, the electrons interact with an external infrared laser pulse in a short undulator, at beam energies typically around 100 MeV. As a consequence of the interaction, the electron beam incoherent energy spread is increased and the microbunching gain suppressed, as suggested by Eq. (1). A LH is routinely adopted at LCLS [14] and FERMI [15] FEL facilities where, in standard operating conditions, ~ 20 and ~ 7 keV, respectively, are added to the 1–3 keV beam incoherent energy spread (all rms values). When the LH is turned off, a high instability gain leads to large coherent optical transition radiation (COTR) signal at screen targets intercepting the time-compressed beam for diagnostic purposes. COTR emission limits the utility of beam profile imaging systems [16,17]. This can be recovered by the LH action which is able to reduce the OTR intensity to the incoherent emission level [11]. The OTR intensity is thus an indicator of the strength of the instability at optical wavelengths. In our experiment, we made use of this relationship, finding agreement of the OTR intensity behavior with numerical and analytical predictions for the instability gain.

We present the first experimental demonstration of magnetically induced phase mixing devoted to suppression

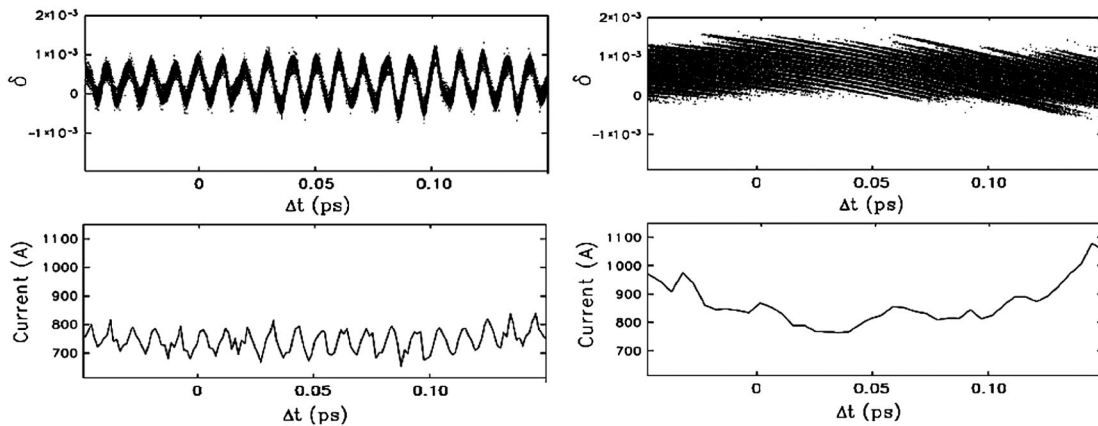


FIG. 1. A 30 μm wavelength, 1% amplitude density modulation is superimposed to an electron beam at 100 MeV. The bunch is then compressed by a factor 10, transported to the entrance of a mixing chicane (left plots) and subjected to phase mixing with $|R_{56}| = 30$ mm. Top row: electron beam longitudinal phase space. Bottom row: current profile. ELEGANT code [22] particle tracking results [19].

of microbunching instability at wavelengths in the optical range and shorter. Initially proposed in [18,19] as an alternative to the beam heating process described above and to other recently proposed schemes in [20,21], phase mixing has the advantage of relying on a relatively simple and robust system, i.e., a four-dipoles, nonisochronous magnetic chicane (hereafter named “mixing chicane”) installed at intermediate linac energies. Although not strictly necessary, the mixing chicane is preferred to be achromatic, like in the case of a symmetric magnetic bunch length compressor. The idea consists in smoothing the electron bunch current and energy distribution by forcing the electrons to “rotate” in the longitudinal phase space (z, δ) , where z is the particle’s longitudinal coordinate along the bunch and δ is the particle’s fractional energy deviation. The rotation is actually a phase slip, primarily induced by the first-order momentum compaction (R_{56}) of the mixing chicane that couples to the (z, δ) correlation established by the upstream instability at its characteristic (short) wavelength scale. This dynamic is illustrated in Fig. 1 [19].

The experiment was carried out at the FERMI S-band linac, which is sketched in Fig. 2. A 500 pC, 2.8 ps rms long electron bunch was photo injected [23] into the linac and time compressed by a factor 12 in a magnetic chicane (BC1) at 0.27 GeV. The second magnetic compressor (BC2) was used as the mixing chicane. The beam was then accelerated to the energy of 1.23 GeV. In general, phase mixing should not affect the bunch length σ_z . This

implies that the correlated fractional energy spread σ_δ evaluated on the bunch length scale (linear energy chirp) has to be small enough to ensure $R_{56}\sigma_\delta \ll \sigma_z$. Bunch length compression in the mixing chicane has also to be avoided because, defeating its scope, it would enhance the total instability gain at short wavelengths, as it happens in a two-stage compression scheme with respect to the one-stage [8,19,24]. If the electron bunch were time-compressed in the early stage(s) of the accelerator, a residual energy chirp, including nonlinear terms, would be present at the mixing chicane, thus potentially inducing bunch length variation. The total chirp would be a result of the linear energy chirp required for previous magnetic compression, the energy spread induced by the rf curvature of the accelerating electric field, the action of linac longitudinal wakefield, and adiabatic damping due to acceleration. The latter two contributions tend to reduce the former. The linac wakefield and the rfcurlvature add quadratic and cubic energy chirp to the beam longitudinal phase space [25]. In order to remove the linear chirp at the BC2 location, the rf phase of two upstream S-band accelerating structures, L3 in Fig. 1, was scanned and set to 140 deg S-band, which is 50 deg off the phase of maximum energy gain. That value gave the minimum horizontal beam size in the middle of BC2, measured with a beam profile imaging system. Beam optics matching upstream of BC2 ensured that the horizontal beam size in the middle of BC2 was dominated by the chromatic particle motion, with estimated contributions to

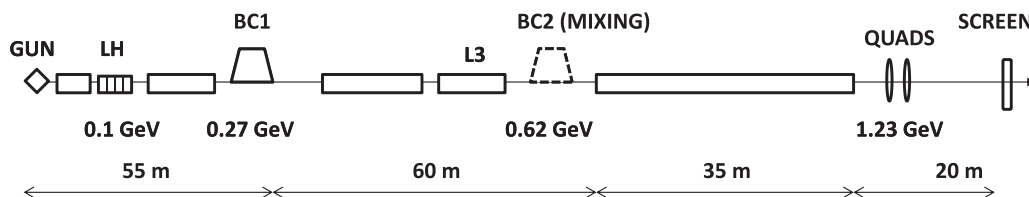


FIG. 2. Sketch of the FERMI linac (not to scale).

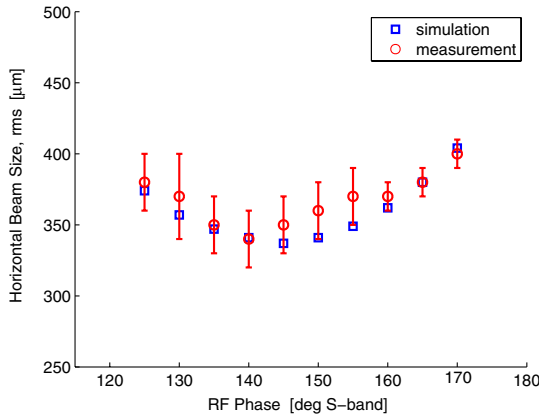


FIG. 3 (color online). Horizontal beam size at the middle of the mixing chicane, BC2, as a function of the rf phase of two upstream accelerating structures (L3 in Fig. 1). The simulation was done with ELEGANT and included CSR and linac geometric wakefields.

the total beam size $\sqrt{\beta_x \varepsilon_x} = 89 \mu\text{m}$ and $\eta_x \sigma_\delta = 319 \mu\text{m}$, $\beta_x = 5 \text{ m}$ being the design betatron function, $\varepsilon_x = 1.6 \text{ nm rad}$ the beam geometric emittance and $\eta_x = 255 \text{ mm}$ the energy dispersion function, all quantities intended in the bending plane and in the middle of BC2. Accordingly, the residual correlated energy spread, now dominated by a quadratic energy chirp, was lowered to 0.1% rms level. Figure 3 shows the agreement between the experimental behavior of the energy-dominated horizontal beam size in BC2 and the particle tracking result, which included geometric wakefields in the accelerating structures. The beam energy at BC2 turned out to be 0.62 GeV. With this linac set up and 90 mrad bending angle in BC2, the ELEGANT code [22] predicts $\sim 10\%$ bunch length variation at the exit of the mixing chicane relative to $\sim 1 \text{ ps}$ full width bunch duration at its entrance.

At the linac's end, an OTR-based beam profile imaging system was used to measure the beam transverse sizes and the beam spot's OTR intensity as the BC2 bending angle was varied in the range 0–90 mrad; $|R_{56}|$ was varying in the range 0–46 mm. During the scan, the beam sizes were kept almost constant at the observation point by tuning upstream quadrupole magnets. The geometric mean of the horizontal and vertical rms beam size had average value of $250 \mu\text{m}$ over the BC2 angle range, with standard deviation of $15 \mu\text{m}$ and peak-to-peak variation of $30 \mu\text{m}$. Beam optics mismatch induced by edge focusing of the mixing chicane's dipole magnets was recovered with a dedicated matching insertion at the linac's end. The effect of CSR emission in BC2 on the beam transverse emittance was counteracted with a manipulation of the beam optics across the chicane [26]. The projected emittance was not varying by more than 10% at the linac's end over the entire BC2 angles' range. The OTR intensity, integrated over the region occupied by the beam spot and averaged over many shots, is shown in Fig. 4 vs the $|R_{56}|$ in BC2, with and without the LH action.

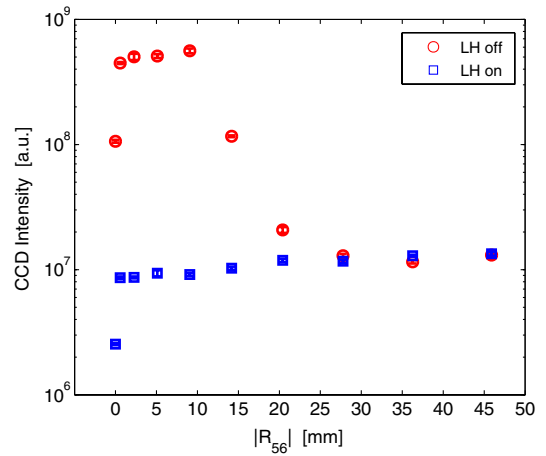


FIG. 4 (color online). Integrated OTR intensity at the FERMI linac's end as a function of $|R_{56}|$ in BC2.

When turned on, the LH provided approximately 50 keV rms incoherent energy spread to the uncompressed beam. Such a strong beam heating was used on purpose since, as discussed below, the analytical model ensures total suppression of microbunching at optical wavelengths and shorter. When the LH was off the OTR intensity increases sharply even for small values of $|R_{56}|$; it then drops for values equal or larger than 9.1 mm. At $|R_{56}| = 27.8 \text{ mm}$, the OTR intensity was the same as in the presence of beam heating. A similar behavior was also observed, in a different preliminary experimental session, with a beam time-compressed in BC1 by a factor 8, whose emitted OTR intensity explored ~ 3 orders of magnitude over the same $|R_{56}|$ range. Moreover, data in Fig. 4 are consistent with those collected at a 5 m downstream OTR screen (not shown). As a revival of microbunching may be expected downstream the linac, the same tuning of the mixing chicane shown in Fig. 4 should be repeated but looking to the OTR intensity at the location of interest. In other words, the optimum strength of phase mixing shall be chosen on the basis of the instability gain for the entire beam line under consideration.

For the case of LH off, we computed the microbunching instability gain at the end of the FERMI linac, at the optical wavelength of 550 nm vs $|R_{56}|$ in BC2, starting from shot noise and on the basis of the linear theory developed in [1–4], for a beam with $1 \mu\text{m}$ transverse normalized emittance and initial 2 keV rms incoherent energy spread. The gain is shown in Fig. 5, left plot. The behavior of the instability gain is in agreement with that of the OTR intensity in Fig. 4 as the instability gain at the optical wavelength of 550 nm (Fig. 5) is suppressed by the same $|R_{56}| \approx 20 \text{ mm}$ that causes drop of the OTR intensity to the incoherent level (Fig. 4). Other two wavelengths at the extremes of the optical range are considered in Fig. 5 to show that, depending on the wavelength of interest, the instability gain is suppressed by a different value of R_{56} . As far as the peak gain is concerned, namely its maximum value evaluated over the entire

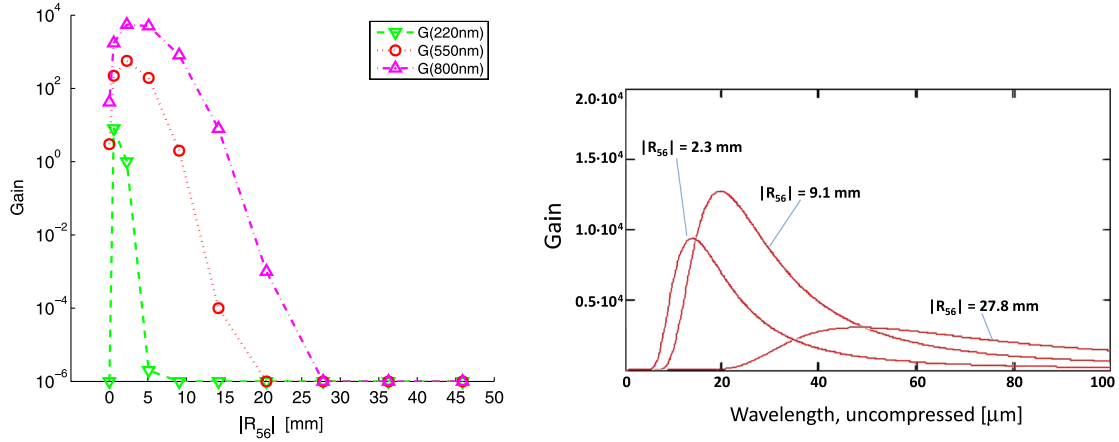


FIG. 5 (color online). Left: analytical evaluation of the microbunching instability gain at the FERMI linac’s end as function of the momentum compaction, $|R_{56}|$, in the mixing chicane (BC2); LH is off. Gain values smaller than 10^{-6} are leveled. Right: analytical evaluation of the microbunching instability gain as function of the initial modulation wavelength, for three values of $|R_{56}|$ in BC2.

spectrum, the analytical model predicts an increase of up to two orders of magnitude as $|R_{56}|$ in BC2 moves from 0 to 46 mm. However, as the momentum compaction is increased and phase mixing becomes more effective, the wavelength of maximum gain redshifts from $1.1 \mu\text{m}$ to $7.1 \mu\text{m}$. This trend is shown in Fig. 5, right plot. Consequently, the amount of phase mixing can be tuned through the mixing chicane’s bending angle to bring the instability gain far enough from the spectral range of interest. With LH on, the optical gain is strongly suppressed for any $|R_{56}|$ in BC2 in the range 0–46 mm and the peak gain is shifted to initial (i.e., uncompressed) wavelengths longer than hundreds of micron (not shown). The experimental behavior of the OTR intensity, as outlined in Fig. 4, confirms the analytical prediction of Fig. 5. This confirmation together with our finding that the instability gain can be controlled with BC2, are the principle results of our study.

We notice a “jump” by a factor ~ 3 of the OTR intensity in Fig. 4 as $|R_{56}|$ in BC2 is moved from 0 to 0.6 mm (10 mrad bending angle). This jump can hardly be explained in terms of microbunching instability because, with LH on, its gain is expected to be largely suppressed at optical wavelengths. Instead, we interpret it through the enhancement of a current spike at the bunch’s edge generated by the strongly non-linear compression induced by BC2 in that bunch region only, in the presence of a quadratic energy chirp. This interpretation is supported by ELEGANT simulations that predict a peak current increasing towards the bunch edges as the beam passes through BC2 (see Fig. 1) and, for the specific set up depicted here, a spike as short as $\sim 1 \mu\text{m}$ appears already at small BC2 angles. The spike would be short enough to emit coherent radiation in the optical range.

In order to investigate the expected performance of magnetic-phase mixing in terms of slice energy spread, we consider three possible locations for the mixing chicane: low, intermediate and high linac energy. Since the process takes advantage of the instability itself to minimize its

impact on the beam *final* longitudinal phase space, the adoption of a mixing chicane at the beginning of the linac, where the bunching has not grown enough yet, inhibits the electrons’ phase slip and is therefore ineffective. Phase mixing at late linac stage smoothes the longitudinal phase space, but the final slice energy spread remains of the same order as the (possibly large) energy modulation amplitude accumulated up to that point (see Fig. 1). These considerations point to the conclusion that phase mixing should take place at an intermediate linac longitudinal coordinate—let us call it \bar{s} —to be most effective. Roughly speaking, for an FEL to be efficient we impose that the energy modulation amplitude accumulated up to \bar{s} and normalized to the final linac energy, be smaller than the so-called FEL parameter, ρ [27]. We then require that the energy modulation amplitude from \bar{s} to the undulator be smaller than that accumulated upstream of the mixing chicane: $\Delta\gamma(\bar{s} \rightarrow s_f) < \Delta\gamma(s_i \rightarrow \bar{s}) < \gamma(s_f)\rho$, with γ the relativistic Lorentz factor. If such an \bar{s} exists, depending on several electron beam and machine parameters, an increase of the slice energy spread will be allowed along the beam line, but not to the extent that it overwhelms the FEL normalized energy bandwidth. Based on this plausible model, the presence of multiple mixing chicanes appears a viable solution in long linacs. We remark that the criterion we are proposing for the production of quasicold electron beams can be verified through the same analytical model [1,2,8,19] used to produce Fig. 5. The model is able to estimate, e.g., energy and density modulation amplitude at any point of the accelerator, thus can be used for finalizing the machine design. For the FERMI moderate one-stage compression, we found that there is no further growth of the instability after phase mixing. The final slice energy spread is then expected to be approximately 100 keV rms (the maximum energy modulation amplitude accumulated up to BC2), which is close to that measured at FERMI during standard operation of the LH [28].

As a by-product of our experimental work we have shown that simultaneous control of the electron bunch length,

energy chirp and bunching factor can be achieved in a reproducible way just as required, e.g., by the two-chicane “compressed harmonic” scheme proposed in [29] to generate coherent x-ray radiation. Preserving coherent microbunching through a two-stage compression system as proposed in [29], however, requires additional optics optimization which is outside the scope of our work. In conclusion, we have demonstrated that magnetic-phase mixing is a viable alternative to the LH in controlling microbunching instability. Tunability of the wavelength at which the microbunching instability gain is suppressed is provided by the chicane’s bending angle, thus ensuring a simple and flexible operation for different machine set-ups. The presence of the mixing chicane imposes a control of the linac rf phases in order to remove the linear energy chirp at its entrance. This control aims at minimizing the correlated energy spread on the scale of the bunch length, and is therefore beneficial, e.g., to FELs. At the same time, it may imply additional rf power, both to cancel the chirp at the mixing chicane and to counterbalance the longitudinal wake potential in the downstream rf structures, while leaving the final beam energy unchanged. In general, the rf budget should also allow one to adjust the energy chirp while the bunch current is changed upstream of the mixing chicane, as this implies a different strength of the linac wakefields. Depending on the linac setting, the additional rf power required for phase mixing may make it a less attractive alternative to a LH. We finally remark that a careful control of higher-order energy chirp, as e.g. reviewed in [25], would help to avoid the production of current spikes at the bunch edges as the beam passes through the mixing chicane and, at the same time, minimize the bunch length variation.

The authors are indebted to L. Badano who provided the calibration curves of the beam profile imaging system; these were used to compute the OTR integrated intensity over all ranges of attenuation. The authors also thank H.-S. Kang for his revision of the script used to compute the instability gain, M. Veronese for instructive discussions about COTR, E. Allaria who inspired the software tool used for data collection, M. Venturini for instructive discussions on topics covered by this Letter, and M. Cornacchia, J. Wu, G. Penco, and R. Bosch, for careful reading and suggestions. We thank the FERMI commissioning team for the time available to carry out the reported measurements. S. D. Mitri and S. Spampinati contributed equally to this work.

*Corresponding author.
simone.dimitri@elettra.eu

- [1] M. Borland *et al.*, *Nucl. Instrum. Methods Phys. Res., Sect. A* **483**, 268 (2002).
- [2] E. L. Saldin, E. A. Schneidmiller, and M. V. Yurkov, *Nucl. Instrum. Methods Phys. Res., Sect. A* **490**, 1 (2002).
- [3] Z. Huang and K. J. Kim, *Phys. Rev. ST Accel. Beams* **5**, 074401 (2002).
- [4] Z. Huang, M. Borland, P. Emma, J. Wu, C. Limborg, G. Stupakov, and J. Welch, *Phys. Rev. ST Accel. Beams* **7**, 074401 (2004).
- [5] T. Shaftan and Z. Huang, *Phys. Rev. ST Accel. Beams* **7**, 080702 (2004).
- [6] R. Akre *et al.*, *Phys. Rev. ST Accel. Beams* **11**, 030703 (2008).
- [7] A. H. Lumpkin, R. J. Dejus, and N. S. Sereno, *Phys. Rev. ST Accel. Beams* **12**, 040704 (2009).
- [8] M. Venturini, *Phys. Rev. ST Accel. Beams* **10**, 104401 (2007).
- [9] M. Venturini and A. Zholents, *Nucl. Instrum. Methods Phys. Res., Sect. A* **593**, 53 (2008).
- [10] Z. Huang *et al.*, *Phys. Rev. ST Accel. Beams* **13**, 020703 (2010).
- [11] S. Spampinati *et al.*, in *Proceedings of the 34th International Free Electron Laser Conference, MOPD58, Nara, Japan, 2012*, <http://accelconf.web.cern.ch/AccelConf/FEL2012/papers/mopd58.pdf>.
- [12] E. Allaria *et al.*, in *Proceedings of the 34th International Free Electron Laser Conference, TUOB02, Nara, Japan, 2012*, <http://accelconf.web.cern.ch/AccelConf/FEL2012/papers/tuob02.pdf>.
- [13] E. L. Saldin, E. A. Schneidmiller, and M. V. Yurkov, *Nucl. Instrum. Methods Phys. Res., Sect. A* **528**, 355 (2004).
- [14] P. Emma *et al.*, *Nat. Photonics* **4**, 641 (2010).
- [15] E. Allaria *et al.*, *Nat. Photonics* **6**, 699 (2012).
- [16] H. Loos *et al.*, in *Proceedings of the 30th Free Electron Laser Conference, THBAU01, Gyeongju, Korea, 2008*, <http://accelconf.web.cern.ch/AccelConf/FEL2008/papers/thbau01.pdf>.
- [17] C. Behrens, C. Gerth, G. Kube, B. Schmidt, S. Wesch, and M. Yan, *Phys. Rev. ST Accel. Beams* **15**, 062801 (2012).
- [18] M. Cornacchia, S. Di Mitri, S. Spampinati, S. V. Milton, in *Proceedings of the 11th European Particle Accelerator Conference, TUPP033, Genoa, Italy, 2008*, <http://accelconf.web.cern.ch/AccelConf/e08/papers/tupp033.pdf>.
- [19] S. Di Mitri, M. Cornacchia, S. Spampinati, and S. Milton, *Phys. Rev. ST Accel. Beams* **13**, 010702 (2010).
- [20] C. Behrens, Z. Huang, and D. Xiang, *Phys. Rev. ST Accel. Beams* **15**, 022802 (2012).
- [21] J. Qiang, C. E. Mitchell, and M. Venturini, *Phys. Rev. Lett.* **111**, 054801 (2013).
- [22] M. Borland, APS Tech, Report No. LS-207, 2000.
- [23] G. Penco *et al.*, *JINST* **8**, P05015 (2013).
- [24] S. Di Mitri, M. Cornacchia, P. Craievich, G. Penco, S. Spampinati, M. Venturini, and A. A. Zholents, in *Proceedings of the 32nd Free Electron Laser Conference, THPB03, Malmö, Sweden, 2010*, <http://accelconf.web.cern.ch/AccelConf/FEL2010/papers/thpb03.pdf>.
- [25] S. Di Mitri and M. Cornacchia, *Phys. Rep.*, doi: 10.1016/j.physrep.2014.01.005 (2014).
- [26] S. Di Mitri, E. M. Allaria, P. Craievich, W. Fawley, L. Giannessi, A. Lutman, G. Penco, S. Spampinati, and M. Trovo, *Phys. Rev. ST Accel. Beams* **15**, 020701 (2012).
- [27] R. Bonifacio, C. Pellegrini, and L. Narducci, *Opt. Commun.* **50**, 373 (1984).
- [28] G. Penco, M. B. Danailov, A. Demidovich, E. Allaria, G. De Ninno, S. Di Mitri, W. M. Fawley, E. Ferrari, L. Giannessi, and M. Trovo, *Phys. Rev. Lett.* **112**, 044801 (2014).
- [29] D. Ratner, A. Chao, and Z. Huang, *Phys. Rev. ST Accel. Beams* **14**, 020701 (2011).